Talanta 79 (2009) 1446–1453

Contents lists available at ScienceDirect

Talanta

journal homepage: www.elsevier.com/locate/talanta

Nonenzymatic glucose voltammetric sensor based on gold nanoparticles/carbon nanotubes/ionic liquid nanocomposite

Hong Zhu, Xiaoqing Lu, Meixian Li, Yuanhua Shao, Zhiwei Zhu *

Institute of Analytical Chemistry, College of Chemistry and Molecular Engineering, Peking University, Beijing 100871, PR China

ARTICLE INFO

Article history:
Received 8 April 2009
Received in revised form 2 June 2009
Accepted 3 June 2009
Available online 12 June 2009

Keywords:
Biosensor
Glucose
Nanocomposite
Gold nanoparticles
Carbon nanotubes
Ionic liquid

ABSTRACT

In this paper, a novel nonenzymatic glucose voltammetric sensor based on a kind of nanocomposite of gold nanoparticles (GNPs) embedded in multi-walled carbon nanotubes (MWCNTs)/ionic liquid (IL) gel was reported. The surface morphology of this nanocomposite was characterized using X-ray photoelectron spectrometer (XPS), scanning electron microscope (SEM) and transmission electron microscope (TEM), respectively. It can be found that most of GNPs lie close to the ektexine of MWCNTs and the others have obviously inserted the inner of MWCNTs through the defects or ends of MWCNTs, due to the attraction between GNPs and MWCNTs as well as the repulsion between GNPs and IL. Voltammetry was used to evaluate the electrocatalytic activities of the nanocomposite biosensor toward nonenzymatic glucose oxidation in alkaline media. The GNPs embedded in MWCNTs/IL gel have strong and sensitive voltammetric responses to glucose, owing to a possible synergistic effect among GNPs, MWCNTs and IL. Under the optimal condition, the linear range for the detection of the glucose is 5.0–120 μM with the correlation coefficient of 0.998, based on the oxidation peak observed during cathodic direction of the potential sweep. The kinetics and mechanism of glucose electro-oxidation were intensively investigated in this system. This kind of nanocomposite biosensor is also highly resistant toward poisoning by chloride ions and capable of sensing glucose oxidation in the presence of 20 μM uric acid and 70 μM ascorbic acid. This work provides a simple and easy approach to the detection of glucose in body fluid with high sensitivity and excellent selectivity.

1. Introduction

Since Clark and Lyons reported the first enzyme electrode in 1962, a variety of experimental improvements on the enzyme-based electrochemical sensors have been reported [1,2]. The historical advances in the development of enzyme-based electrochemical glucose sensors commenced with Updike and Hicks reporting the first enzyme-based amperometric glucose sensor in 1967 [3]. The glucose sensors of the first and the second generation employ oxygen and artificial mediators as an electron mediator between glucose oxidase and electrode surface, respectively, while the third generation is based on the strategy of the direct electron transfer between enzyme and electrode. But the most common and serious problems with enzymatic glucose sensors are insufficient long-term stability and unsatisfactory reproducibility originating from the nature of the enzymes as well as the activity of the immobilized enzymes [4]. As a result, the nonenzymatic glucose sensor keeps coming closer to practical applications than enzymatic one.

However, the nonenzymatic direct oxidation of glucose on some traditional electrodes including C, Cu, Ni, Fe, Pt and Au electrodes has also two key problems, one is the low sensitivity due to the sluggish kinetics of glucose electro-oxidation that bring about poor faradic response, the other is the poor selectivity resulting from both chemisorbed intermediates that block the electroactive surface, and various endogenous species such as ascorbic acid and uric acid that can also be oxidized in the potential range of glucose oxidation. Basically, roughness of nanoscopic dimensions can be used to selectively enhance the faradic current of a sluggish reaction. Based on this principle, Park et al. [5] constructed mesoporous structures on the surfaces of pure platinum electrodes responding more sensitively to glucose than to common interfering species. With new nanomaterials being reported continually in this nanoera, the development of nonenzymatic glucose sensor can be accelerated by the application of nanomaterials [4].

Of all the nanomaterials, metal nanoparticles and carbon nanotubes (CNTs) are of great interest for nonenzymatic glucose sensor because of their extraordinary physicochemical characteristics. For example, GNPs [6,7], nanoporous platinum [8], and highly ordered platinum-nanotubule [9] have been used for direct glucose sensing. Nanoporous Pt–Pb networks [3], Au–Pt alloy nanoparticles [10] and homogeneously bimetallic Au_mAg_{100-m} nanoparticles [11,12] have

* Corresponding author. Tel.: +86 10 62757953; fax: +86 10 62751708.
E-mail address: zwzhu@pku.edu.cn (Z. Zhu).

0039-9140/$ – see front matter © 2009 Elsevier B.V. All rights reserved.
doi:10.1016/j.talanta.2009.06.010

also showed improvements in electrocatalytic activity for glucose. In addition, since CNTs were used to directly detect oxidation of glucose in 2004 [13], freestanding single-wall CNTs [14] and restructured CNTs forest [15] have found applications in constructing highly sensitive, stable, and fast response glucose sensors.

The performance of biosensors for sensitive and selective detection of glucose has been constructed by incorporating catalytic metal or alloy nanoparticles such as highly dispersed Pt nanoparticles [16], BO nanoparticles [17], Cu nanoclusters [18], Pt–Pb alloy nanoparticles [19] and even MnO_2 [20] to CNTs. Actually, the so-called bucky gel not like ordinary organogels or hydrogels, that is a kind of mixture of CNTs and room-temperature IL, discovered by Fukushima in 2003 [21], can also be used to detect glucose directly [22], but the sensitivity with the detection limit of 1.0 mM is still a problem. However, because IL has some advantages such as wide potential windows, good conductivity and fine chemical stability, the most important is that it can be designed by choosing specific cations and anions to meet specific requirements, the bucky gel has captured the attention of the analysts in different analytical applications [23–30]. Since GNPs have been successfully used to decorate CNTs for glucose sensing in attempts to improve sensor performance, the addition of it to bucky gel may be worth of trying. Furthermore, Wang's research results indicate that modification of MWCNT with IL and GNPs could play an important role in increasing the electrocatalytic activity of MWCNT to oxygen [31]. So the motivation for this study is derived primarily from the anticipation of a synergistic electrocatalytic benefit to glucose from the combined properties of nanocomposite made of GNPs, MWCNTs and IL. In this report, a novel nonenzymatic glucose voltammetirc sensor based on this nanocomposite was prepared and characterised. Compared with other similar sensors, it has higher sensitivity and better selectivity owing to intrinsic synergistic effect of this nanocomposite. For example, the detect limit of 2.0 μM is better than some reference reports [7,32]. Actually, each constituent in this nanocomposite plays a key role in sensing glucose. In brief, GNPs are the cores of this nanocomposite, surrounded by MWCNTs as support for GNPs. IL acts as bridges connecting GNPs/MWCNTs one another with bucky gel as platform for the whole nanocomposite.

2. Experimental

2.1. Materials

D-Glucose and hydrogen tetrachloroaurate (III) trihydrate ($HAuCl_4{\cdot}3H_2O$, 99.9%) were purchased from Sigma–Aldrich. Sodium citrate and uric acid (UA) were used as received from Merck. L(+)-Ascorbic acid (AA) was purchased from Northeast Pharmacy Institute of China. The MWCNTs with mean diameter of about 30 nm were obtained from the Tsinghua University of China as gifts. They were produced by catalytic chemical vapor deposition (CCVD) method, and the details of synthesis were reported elsewhere [33,34]. The ionic liquid of 1-(4-sulfonylbutyl)-3-methylimidazole hexafluorophosphate was provided by Lanzhou Institute of Chemical Physics as gift, and the details of synthesis method were reported [35]. The purities of MWCNTs and IL are both more than 99%. Triply distilled water was used to prepare all solutions. Highly purity nitrogen was used for deaeration. All other chemicals were analytical grade and were used as received from commercial sources. The human blood serum was obtained from Campus Hospital of Peking University.

2.2. Apparatus

The XPS were recorded on a AXIS Ultra X-ray photoelectron spectrometer, using monochromatized Al Kα X-ray as the excitation source and choosing C 1s (284.6 eV) as the reference (Kratos, UK). The SEM measurements were performed on a Strats DB235 FIB scanning electron microscope (Phlips-FEI, USA). The TEM images were obtained using Tecnai F30 transmission electron microscope (Phlips-FEI, Holland). Electrochemical measurements were performed with a CHI 660C electrochemical workstation (Shanghai, China). A standard three-electrode electrochemical cell was used. The electrode assembly consisted of a bare or a "thick" or a "thin" glassy carbon electrode (GCE) as the working electrode, a platinum wire as the counter electrode and Ag/AgCl (3 M KCl) as the reference electrode. The potential in all figures are indicated relative to this reference electrode. All solutions were deaerated with highly purified nitrogen before electrochemical measurements, and nitrogen was passed over the top of the solution during the experiments. All measurements were conducted at room temperature ($25 \pm 2^{\circ}C$).

2.3. Preparation of GNPs solution

GNPs were prepared based on Frens' method [36]. Briefly, 15 mL of 38.8 mM sodium citrate was rapidly added into 150 mL of boiled 1 mM aqueous solution of $HAuCl_4$ under intensive stirring. The solution was boiled for several minutes until its color was changed from yellow to colorless, then dark blue, dark red and finally red wine color. At this moment the solution was cooled. The obtained suspension of GNPs was stored at room temperature and used within several days. The concentration of this prepared GNPs solution was about 1 mM, and their mean diameter estimated by SEM was about 10 nm.

2.4. Preparation of nanocomposites

It is difficult for GNPs to be dispersed well in ordinary bucky gel like MWCNTs/IL of 1-octyl-3-methylimidazolium hexafluorophosphate we used previously [25]. For solving this problem, carboxylated MWCNTs and water-soluble IL of 1-(4-sulfonylbutyl)-3-methylimidazole hexafluorophosphate were used to prepare new bucky gel. Strictly, this gel should be called bucky solution because of its good solubility. The preparation method used in carboxylating MWCNTs is similar to the report [37]. Nanocomposite *a* was prepared by adding 4 mL of GNPs solution and 10 mg of MWCNTs into 100 mg of IL with ultrasonic agitation for 10 min. For comparative investigations, nanocomposites *b–e* without GNPs or MWCNTs or without IL in them were prepared based on similar method. Table 1 shows the compositions of those nanocomposites.

2.5. Fabrication of electrochemical sensor

Prior to use, a GCE with a diameter of 4 mm was polished with 0.05 μm alumina slurry, and then washed ultrasonically in distilled water and ethanol for a few minutes, respectively. After that, the well-polished GCE was coated by casting 2.0 μL of the as-

Table 1
The compositions of nanocomposites and their XPS characterization results.

	Nanocomposite code				
	a	*b*	*c*	*d*	*e*
Compositions					
GNPs (mL)	4	–	4	4	4
MWCNTs (mg)	10	10	–	10	1
IL (mg)	100	100	100	–	10
H_2O (mL)	–	4	–	–	–
Real Au content (%)	0.7	0	0.8	7	7
XPS					
Apparent Au content (%)	0	0	0.2	0	0.1
Imine N fraction in total N of IL (%)	92	92	86	–	62

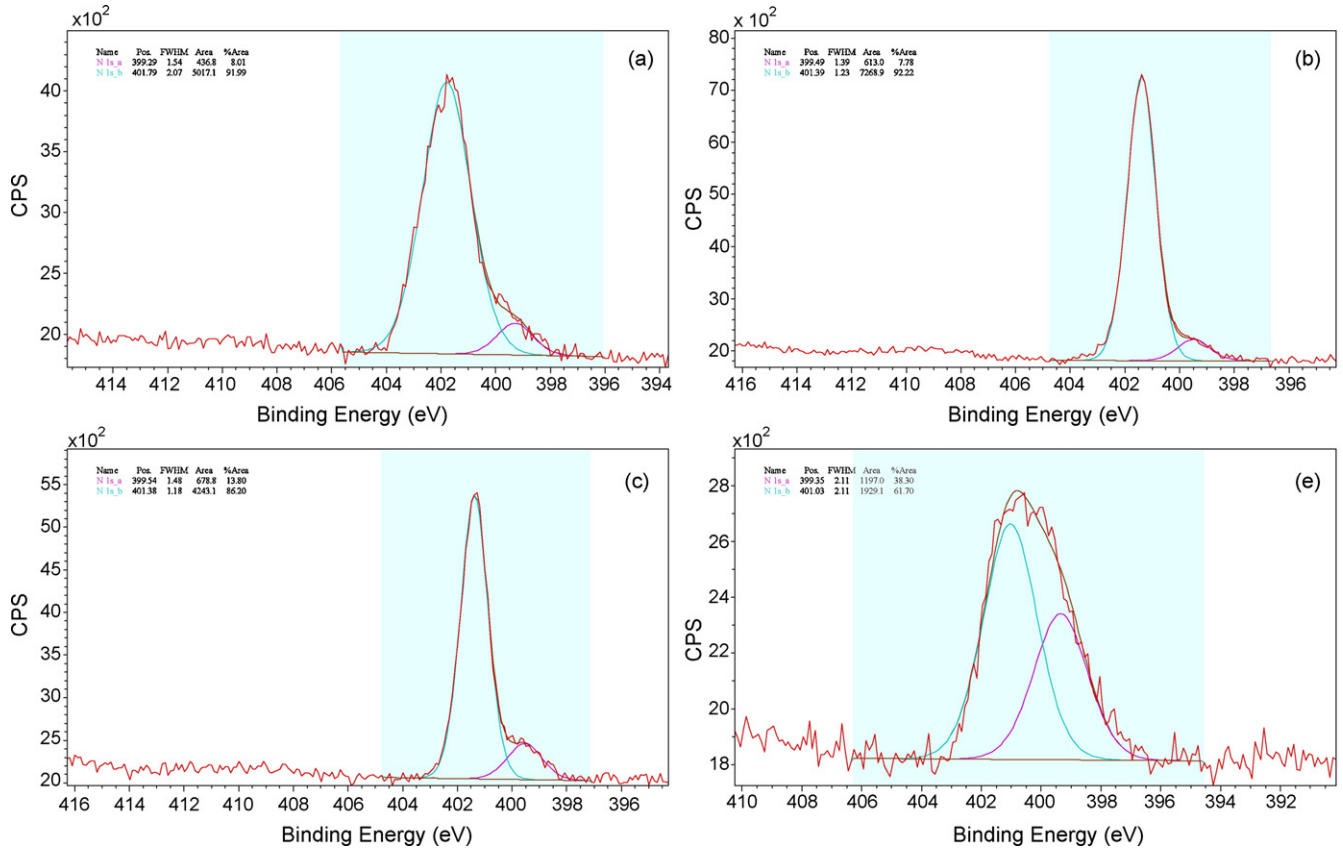

Fig. 1. N $1s_{a-b}$ XPS patterns of nanocomposites containing IL. (a) GNPs/MWCNTs/IL; (b) MWCNTs/IL; (c) GNPs/IL; (e) GNPs/MWCNTs/IL containing much more GNPs. See Table 1 in detail.

prepared nanocomposite or 2.0 μL of the diluted nanocomposite solution, and dried under an infrared lamp. The coating amount of nanocomposite has proven to play a key role in sensing different concentrations of glucose electro-oxidation. For convenience in discussion, "thick" and "thin" GCE were denominated corresponding to the coating amount being 100% and 5% of the prepared nanocomposite, respectively.

3. Results and discussion

3.1. Characterization of nanocomposites

The prepared nanocomposites were characterized by XPS, SEM and TEM, respectively. Table 1 shows their compositions and XPS characterization results in detail. From the XPS patterns (Fig. 1), the noticeable phenomena are related to detectable amounts of Au and N in nanocomposites. For example, the apparent Au contents (about 0.1%) in nanocomposites *d* and *e* are much lower than their real values (7%). Though the limited detection range of XPS cannot be neglected, it still implies that the most of GNPs have been hidden. Obviously, the inner of MWCNTs should be the likeliest burrow for GNPs with mean diameter of 10 nm. The following SEM and TEM images would support such a hypothesis that some of GNPs can be embedded into MWCNTs. As shown in Fig. 1, the prepared nanocomposites containing IL (except nanocomposite *d*) include two types of N: amine and imine, corresponding to the XPS binding energy located at 401 and 399 eV, respectively. The pi-pi conjugation between imidazole ring in IL and MWCNTs facilitates the N conversion from amine to imine [22], which makes imine N fraction in total N of IL increase from 86% (nanocomposite *c*) to more than 90% (nanocomposites *a* and *b*). However, large quantities of GNPs play a negative role in this kind of conversion, and their presence makes imine N fraction decrease rapidly to 62% (nanocomposite *e*). These results indicate that there are interactions among GNPs, MWCNTs and IL.

These nanocomposites' typical morphologies are shown in Figs. 2 and 3. From SEM and TEM images of nanocomposite *b*, it can be found that IL as a good dispersant makes entangled MWCNTs untangled. GNPs in nanocomposite *a* cannot be clearly observed by SEM in either 100 nm or 50 nm scale. In contrast, the SEM image of nanocomposite *e* shows large quantities of GNPs because the amount of Au in nanocomposite *e* almost decuples nanocomposite *a*. If no MWCNTs in nanocomposite like nanocomposite *c*, almost all of GNPs aggregate, which implies the repulsion interaction between GNPs and IL. As far as nanocomposite *d* without IL is concerned, its SEM image shows GNPs attach to the outer wall of MWCNTs due to attraction.

Compared with SEM, TEM can provide clearer information regarding the surface morphologies of these nanocomposites. From the TEM images of nanocomposites *a* and *e*, it can be found that most of GNPs attach to the outer wall of MWCNTs and that some are embedded into the inner of MWCNTs. In the absence of MWCNTs, GNPs aggregate altogether like "islands" in the ocean of IL. While in the absence of IL, GNPs attach to the outer wall of MWCNTs.

Based on the above results, the following conclusions can be drawn: First, entangled MWCNTs are dispersed well in IL owing to the pi-pi conjugation between imidazole ring in IL and MWCNTs. Second, the synergetic effects including repulsion between GNPs and IL as well as attraction between GNPs and MWCNTs, make most of GNPs attach to the outer wall of MWCNTs and some of GNPs be embedded into the inner of MWCNTs.

Fig. 4 shows the schematic illustration of nanocomposite *a* (GNPs/MWCNTs/IL). Each component has its specific function. Meanwhile, there are complicate interactions among them. In brief, GNPs are regarded as cores of nanocomposite, MWCNTs as support

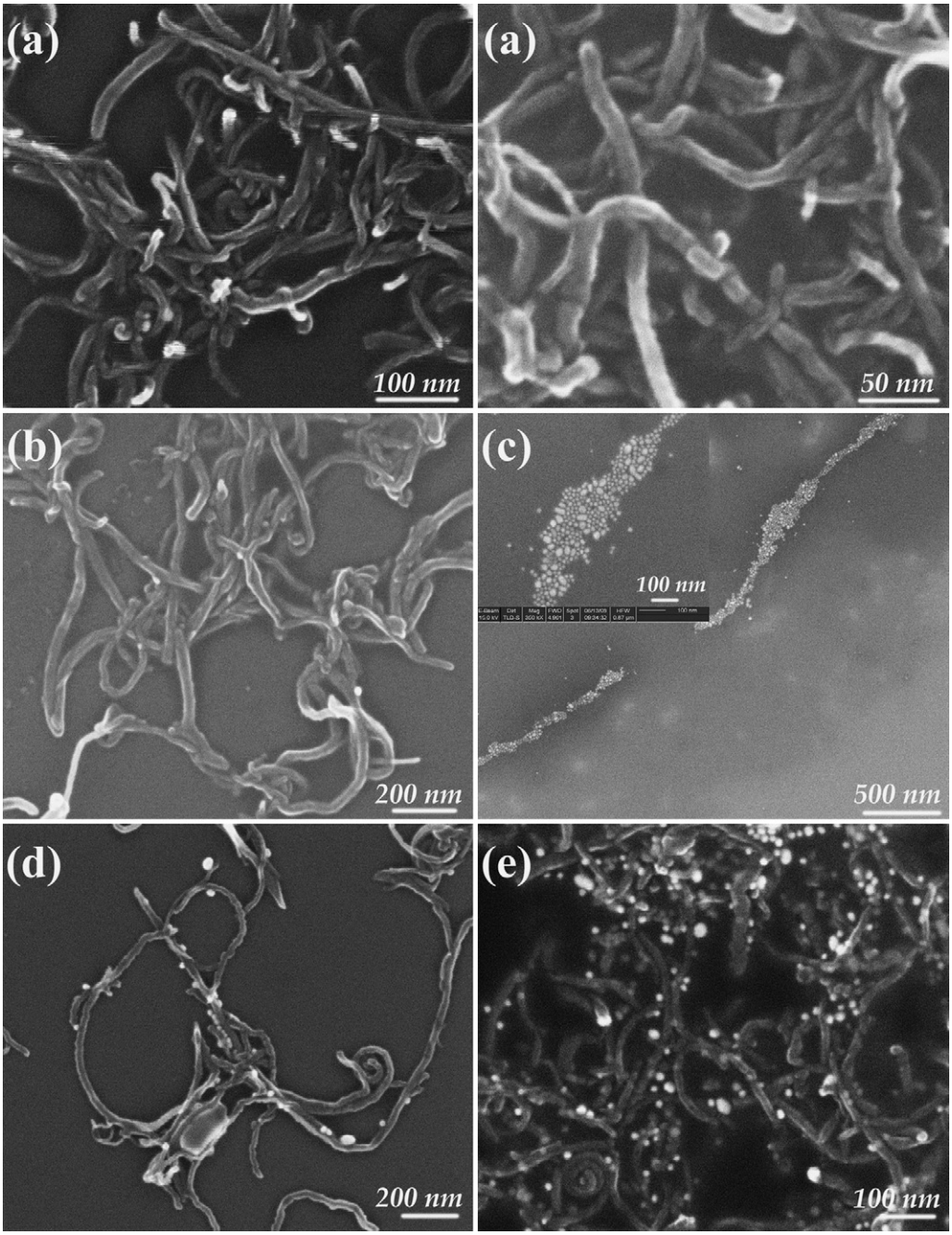

Fig. 2. SEM images of the nanocomposites. (a) GNPs/MWCNTs/IL with different magnifications; (b) MWCNTs/IL; (c) GNPs/IL; (d) GNPs/MWCNTs; (e) GNPs/MWCNTs/IL with much more GNPs.

for GNPs, IL as bridge connecting GNPs/MWCNTs one another and bucky gel as platform for the whole nanocomposite. This makes possible the application of such a nanocomposite for glucose analysis.

3.2. Characterization of nanocomposites electrochemical sensor

Though nanocomposite *a* is a water-soluble composite, the stability of GCE modified with it is very good in alkaline media (more than 12 h). This phenomenon differing from expectation implies that this kind of GNPs-embedded bucky solution still has excellent adhesion to GCE. The electrochemical impedance spectroscopy (EIS) can give useful information of the impedance changes on the electrode surface before and after modification. Basically, the EIS includes a semicircular part at higher frequencies and a linear part at lower frequencies, which correspond to the electron transfer limited process and the diffusion process, respectively. Additionally the diameter of semicircular is equivalent to the charge transfer resistance (R_{ct}). The results of EIS show the significant differences between the bare GCE and modified electrode in the presence of equimolar $[Fe(CN)_6]^{3-/4-}$. The semicircular for the bare GCE cannot be observed due to very low R_{ct}. After GCE was modified by GNPs/MWCNTs/IL nanocomposite, R_{ct} increased markedly to 125 Ω. It seems to indicate that the coated nanocomposite film acts as a barrier and blocks interfacial charge transfer. Actually, this R_{ct} value of 125 Ω is much lower than ordinary modified electrode, which means GNPs/MWCNTs/IL nanocomposite has good conductivity. Together with their good biocompatibility, this further makes possible the application of such a nanocomposite for glucose sensing.

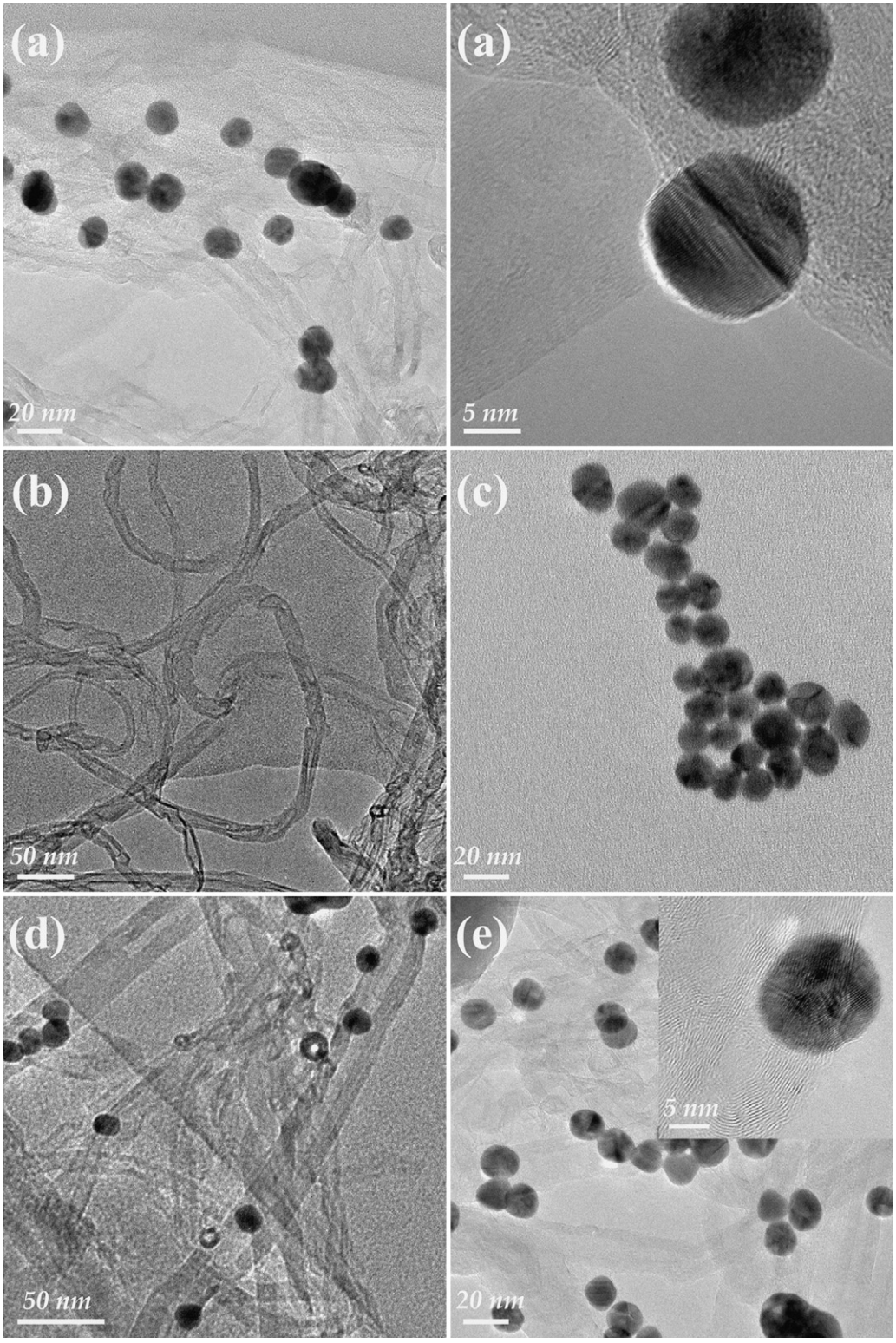

Fig. 3. TEM images of the nanocomposites. (a) GNPs/MWCNTs/IL with different magnifications; (b) MWCNTs/IL; (c) GNPs/IL; (d) GNPs/MWCNTs; (e) GNPs/MWCNTs/IL with much more GNPs.

3.3. Electrochemical behavior of glucose at the prepared nanocomposite GCE

Voltammetric methods were used to investigate and compare the catalytic activities of the as-prepared nanocomposite GCE to glucose electro-oxidation. From the cyclic voltammograms (CVs) of the prepared MWCNTs/IL (nanocomposite *b*) GCE and GNPs/IL (nanocomposite *c*) GCE measured in 0.02 M NaOH solution in the absence or the presence of glucose, no other obvious redox peak appears at GNPs/IL GCE except a small reduction peak at about −0.40 V after the concentration of glucose is increased to 0.3 mM. The similar reduction peak can also be observed at MWCNTs/IL GCE. Based on our previous results, this small but clear reduction peak should be due to the reduction of the oxidized products of

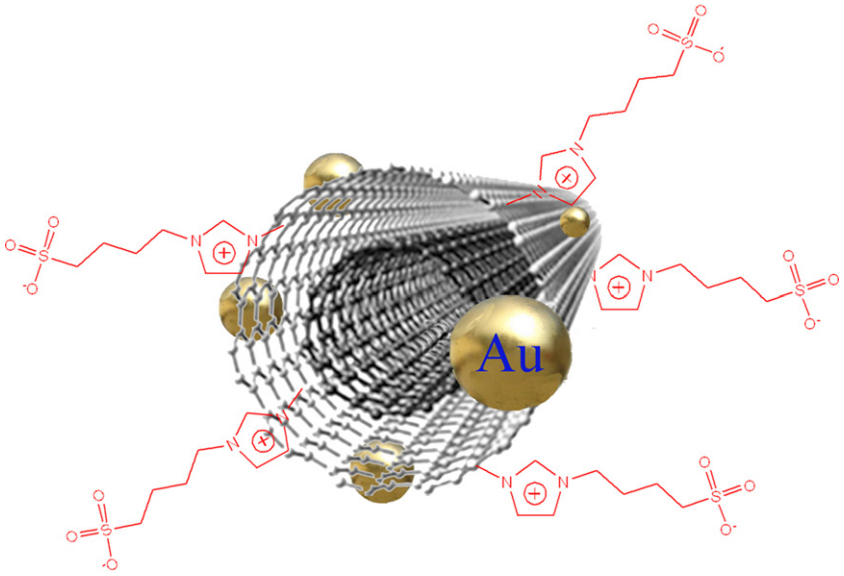

Fig. 4. Schematic illustration of nanocomposite *a* (GNPs/MWCNTs/IL).

glucose (gluconic acid or its derivatives) [22]. Unfortunately, its low sensitivity is not available for glucose analysis.

The addition of GNPs into MWCNTs/IL would bring about great changes of the redox of glucose because that may take advantage of high surface area and good electrocatalytic activity of both MWCNTs and GNPs. Two alkaline solutions (0.02 M and 0.1 M NaOH) in favor of glucose oxidation were chosen as supporting electrolyte to investigate electrochemical behavior of glucose at the prepared GNPs/MWCNTs/IL GCE. As shown in dashed curve of Fig. 5A, the CV curve of "thick" GCE measured in 0.02 M NaOH demonstrates typical gold oxidation/reduction behavior usually associated to formation and reduction of gold oxide [7], which corresponds to P_{a3} at 0.550 V and P_c at 0.083 V, respectively. In the presence of glucose, besides two additional oxidation peaks (P_{a1} at −0.265 V and P_{a2} at 0.148 V) appearing in the anodic potential sweep, another oxidation peak showing much more pronounced glucose oxidation currents appears at 0.091 V (P'_a) during the potential sweep in the cathodic direction (Fig. 5, curves *b–f*). Obviously, this peak is overlapped with the reduction peak of gold oxide (P_c). However, the peak currents were found to be linearly dependent on the glucose concentration ranging from 0.050 mM to 2.0 mM with the correlation coefficient of 0.996. This linear dependency can be used as calibration for analytical application.

Kurniawan et al gave the physical reason for the appearance of oxidation peak during cathodic direction of the potential sweep by investigating the electrical blockage of the electrode surface by nonconductive gold oxide forming at higher potentials [7]. This effect may be much more significant due to the introduction of GNPs, because formation of insulating gold oxide on GNPs surfaces leads to longer tunneling distance and therefore to higher resistance. As far as GNPs/MWCNTs/IL system is concerned, the case is a bit different from the above. In spite of poor conductivity of gold oxide, good conductivities of MWCNTs and IL would not bring about obvious increase of resistance, as indicated by EIS experiment. In fact, the catalytic effect of the GNPs mixed in the bucky gel can also be rationalized by considering the incipient hydrous oxide/adatom mediator model [32,38]. The electro-oxidation of glucose strongly depends on the number of active GNPs, and the untangled MWCNTs owing to the existence of IL can lead to dramatical augmentation of the number. The microenvironment consisting of GNPs, MWC-

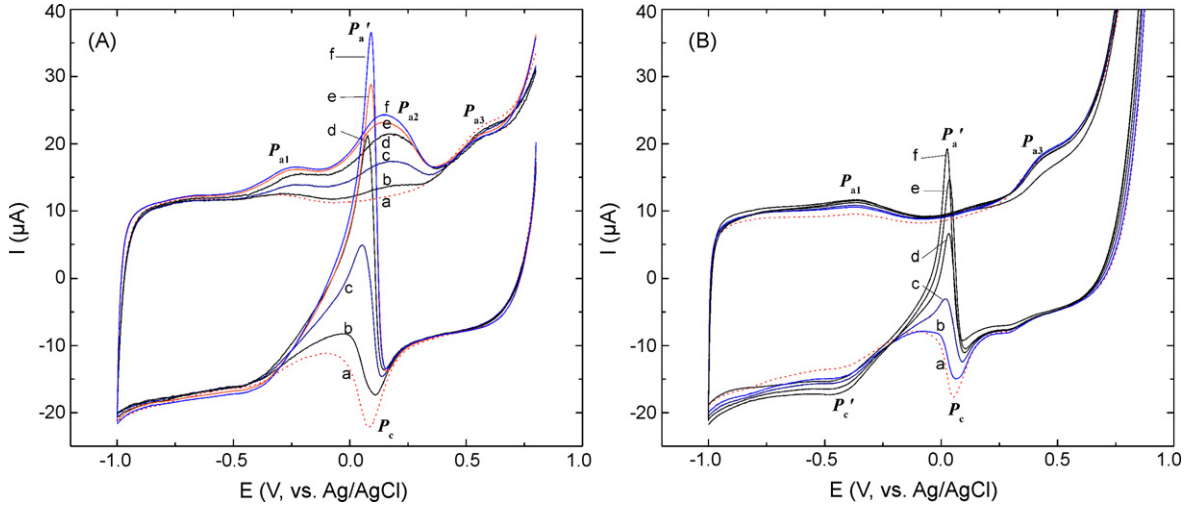

Fig. 5. CVs in the absence (dashed curve) or the presence of glucose (solid curve) at "thick" GCE. Scan rate: 100 mV/s. Supporting electrolyte: (A) 0.02 M NaOH solution; (B) 0.1 M NaOH solution. The concentration of glucose (mM): (a) 0; (b) 0.1; (c) 0.5; (d) 1.0; (e) 1.4; (f) 1.8.

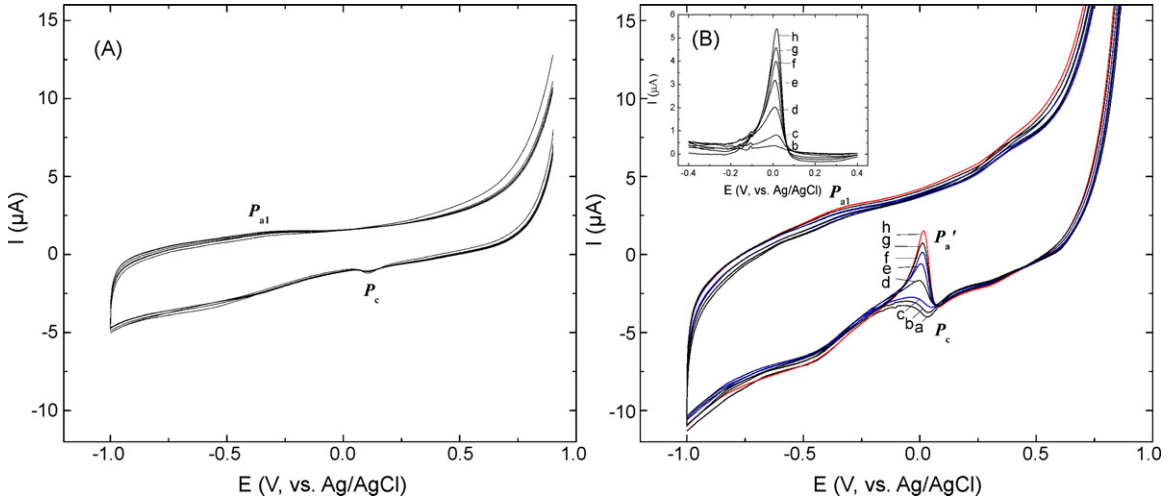

Fig. 6. CVs in the absence or the presence of glucose at "thin" GCE. Scan rate: 100 mV/s. Supporting electrolyte: (A) 0.02 M NaOH solution; (B) 0.1 M NaOH solution. The concentration of glucose (μM): (a) 0; (b) 5.0; (c) 15; (d) 35; (e) 55; (f) 75; (g) 95; (h) 115. Inset: voltammograms with correction of background current for different concentrations of glucose at "thin" GCE.

NTs, IL and alkaline media is propitious to the redox of glucose. The P_{a1} shown in Fig. 5 should result from the electrosorption of glucose to form adsorbed intermediate, releasing one proton per glucose molecule. With the accumulation of the intermediates in the nanocomposite, the further oxidation of glucose is inhibited because the most of active GNPs being occupied. However, with the potential moving to more positive values, formation of OH_{ad} occurs by the partial discharge of OH^-, which can promote the oxidation of those poisoning intermediates. Free and active GNPs are released for the direct oxidation of glucose and the P_{a2} is formed. When the potential moving to more than 0.37 V, the P_{a3} shows up due to the oxidation of gold to gold oxide, followed by the decrease in number of active GNPs. In the reverse potential sweep, with the reduction of gold oxide (P_c), in an instant a great deal of free active GNPs are formed once again, which dramatically facilitates the direct oxidation of glucose, resulting in a sharp oxidation peak (P_a').

Compared with Fig. 5A, the CV signals observed in 0.1 M NaOH solution are essentially different (Fig. 5B). More basic condition causes shifts of all peak potentials toward negative direction. In three oxidation peaks concerning glucose, only P_a' still keeps sharp peak shape but a slight decrease of peak current, while P_{a1} shows weak peak current and P_{a2} disappears. More interestingly, an additional reduction peak (P_c') appears at about −0.45 V, which should be due to the reduction of the oxidized products of glucose (gluconic acid or its derivatives), because this peak is only apparent in the presence of glucose. Obviously, its sensitivity is better than the one observed with GNPs/IL GCE or MWCNTs/IL GCE. We suppose that more basic media has more effects on the oxidation of gold than glucose. This means less active GNPs are available for the electro-oxidation of glucose, resulting in low oxidation peak currents of glucose.

The thickness of the nanocomposite coating film has great impact on the electrochemical properties of GNPs/MWCNTs/IL GCE. If "thin" GCE being used to investigate the electrochemical behavior of glucose as indicated in Fig. 6, more basic media would be chosen as the optimal condition for detection of low concentrations of glucose. Unlike "thick" GCE, thinner nanocomposite coating film can bring about more effectively active GNPs owing to the exposure of free GNPs. Meanwhile, stronger basic condition is propitious to removal of the oxidation products of glucose like glucolactone from the nanocomposite. Glucolactone can be hydrolyzed under this condition, and this hydrolysis further promotes the recovery of active GNPs in an instant, resulting in more sensitive glucose oxidation peak current (P_a') shown in Fig. 6B. On the contrary, gentle basic condition has no obvious effect on the electro-oxidation of low concentration of glucose. As shown in Fig. 6A, during cathodic direction of the potential sweep no oxidation peak can be observed except the reduction peak of gold oxide (P_c). The inset shows the voltammograms in 0.1 M NaOH solution for different concentrations of glucose after correction of background current. The corrected peak currents are linearly dependent on the glucose concentration ranging from 5.0 μM to 120 μM with the correlation coefficient of 0.998. The detect limit is found to be as low as 2.0 μM based on the signal-to-noise ratio of 3. This linear dependency can be used as calibration for high-sensitivity analytical application of glucose.

The corrected peak currents of P_a' increase linearly with the square root of the scan rate in the range of 0.01–0.6 V/s. After washing the electrode with a large amount of triply distilled water and afterwards putting it in a blank solution (0.1 M NaOH), no oxidation peak appears in the negative potential sweep. These results show that glucose is hardly adsorbed at the surface of "thin" GCE and that the electrode reaction is controlled by the diffusion of glucose in the solution. Meanwhile, this also indicates that the faradic response of a sluggish reaction like glucose oxidation would be significantly improved by the GNPs embedded in MWCNTs/IL bucky gel. On the other hand, the corrected peak potential of P_a' is affected strongly by the reduction peak potential of gold oxide (P_c). It is reasonable that the peak potential of P_c is followed by P_a' as the oxidation of glucose is based on free GNPs. With the increase of potential scan rate, both the peak potentials of P_a' and P_c move to more negative values, while the peak current of P_a' first increases and then decreases after its peak potential below 0 V. It can be explained by the fact that when the potential is below around 0 V, the second oxidation of glucose corresponding to P_{a1} would not occur, hence low peak current would be observed.

3.4. Voltammetric detection of glucose by "thin" GCE

There are many reports regarding amperometric sensing applications of glucose by measuring current response at a fixed potential and within a certain time after adding the analyte and possible interfering species [3,16,32]. In this paper, voltammetric response of "thin" GCE in 0.1 M NaOH solution has been regarded as the optimal mode for the high-sensitivity detection of glucose in body fluid. In order to verify the performance of this nonenzymatic

Table 2
Experimental results for the determination of glucose in human blood serum.

No.	Glucose spiked (mM)	Glucose found (mM)	Recovery (%)
1	–	5.4	–
2	10.0	14.6	92
3	20.0	24.0	93

glucose voltammetric sensor based on "thin" GCE, some possible interfering species like AA, UA and Cl^- were added into sample solution. Based on our experiments, the presence of 70 μM AA, 20 μM UA and 40 μM Cl^- doesn't interfere in the detection of 40 μM glucose by standard of decrease in peak current response lower than 5%. The normal physiological level of glucose (3–8 mM) in serum is much higher than those of AA (0.1 mM) and UA (0.02 mM), also higher than Cl^- (2.7 mM). Additionally, the fact that the peak of glucose oxidation is observed at the cathodic direction of the potential sweep especially facilitates the decrease of the number of possible interferents. Thus, it is clear that this "thin" GCE would give higher sensitivity and selectivity for glucose detection. However, proteins have effects on the electrochemical response of "thin" GCE owing to their strong adsorption to the electrode surface. It is necessary to remove them from sample when "thin" GCE is used to detect glucose in real samples. Table 2 shows experimental results for the determination of glucose in human blood serum.

4. Conclusions

A quick, simple and sensitive electrochemical biosensor has been developed for glucose detection based on the application of such a novel nanocomposite consisting of GNPs, MWCNTs and IL. GNPs embedded in MWCNTs/IL bucky gel show good electrocatalytic activity to glucose oxidation at the cathodic direction of the potential sweep, owing to some synergistic effects among GNPs, MWCNTs and IL. This has been used in the determination of glucose in human blood serum with satisfactory result. The simplicity, stability and durability make "thin" GCE a very good platform for biosensors. Moreover, combining the environment-friendly and designable ionic liquid with nanomaterials having excellent electrochemical characteristics may be a new idea for developing some novel and powerful biosensors.

Acknowledgements

This work was supported by the National Natural Science Foundation of China (NSFC, Nos. 20305001; 20675005 and 20735001).

References

[1] K. Wang, J.J. Xu, D.C. Sun, H. Wei, X.H. Xia, Biosens. Bioelectron. 20 (2005) 1366.
[2] S.K. Kang, R.A. Jeong, S. Park, T.D. Chung, S. Park, H.C. Kim, Anal. Sci. 19 (2003) 1481.
[3] J. Wang, D.F. Thomas, A. Chen, Anal. Chem. 80 (2008) 997.
[4] S. Park, H. Boo, T.D. Chung, Anal. Chim. Acta 556 (2006) 46.
[5] S. Park, T.D. Chung, H.C. Kim, Anal. Chem. 75 (2003) 3046.
[6] M. Tominaga, T. Shimazoe, M. Nagashima, I. Taniguchi, Electrochem. Commun. 7 (2005) 189.
[7] F. Kurniawan, V. Tsakova, V.M. Mirsky, Electroanalysis 18 (2006) 1937.
[8] C.H. Chou, J.C. Chen, C.C. Tai, I.W. Sun, J.M. Zen, Electroanalysis 20 (2008) 771.
[9] J.H. Yuan, K. Wang, X.H. Xia, Adv. Funct. Mater. 15 (2005) 803.
[10] M. Tominaga, T. Shimazoe, M. Nagashima, I. Taniguchi, Chem. Lett. 34 (2005) 202.
[11] M. Tominaga, T. Shimazoe, M. Nagashima, I. Taniguchi, J. Electroanal. Chem. 615 (2008) 51.
[12] M. Tominaga, T. Shimazoe, M. Nagashima, H. Kusuda, A. Kubo, Y. Kuwahara, I. Taniguchi, J. Electroanal. Chem. 590 (2006) 37.
[13] J.S. Ye, Y. Wen, W.D. Zhang, L.M. Gan, G.Q. Xu, F.S. Sheu, Electrochem. Commun. 6 (2004) 66.
[14] J.X. Wang, X.W. Sun, X.P. Cai, Y. Lei, L. Song, S.S. Xie, Electrochem. Solid State Lett. 10 (2007) J58.
[15] C.K. Tan, K.P. Loh, T.T. Johnb, Analyst 133 (2008) 448.
[16] L.Q. Rong, C. Yang, Q.Y. Qian, X.H. Xia, Talanta 72 (2007) 819.
[17] Y.L. Wang, D.D. Zhang, W.W. Zhang, F. Gao, L. Wang, Anal. Biochem. 385 (2009) 184.
[18] X.H. Kang, Z.B. Mai, X.Y. Zou, P.X. Cai, J.Y. Mo, Anal. Biochem. 363 (2007) 143.
[19] H.F. Cui, J.S. Ye, X. Liu, W.D. Zhang, Nanotechnology 17 (2006) 2334.
[20] J. Chen, W.D. Zhang, J.S. Ye, Electrochem. Commun. 10 (2008) 1268.
[21] T. Fukushima, A. Kosaka, Y. Ishimura, T. Yamamoto, T. Takigawa, N. Ishii, T. Aida, Science 300 (2003) 2072.
[22] Y. Zhao, H. Liu, Y. Kou, M. Li, Z. Zhu, Q. Zhuang, Electrochem. Commun. 9 (2007) 2457.
[23] T. Fukushima, T. Aida, Chem.-Eur. J. 13 (2007) 5048.
[24] Y.F. Zhao, T.L. Ye, H. Liu, Y. Kou, M.X. Li, Y.H. Shao, Z.W. Zhu, Q.K. Zhuang, Front. Biosci. 11 (2006) 2976.
[25] Y.F. Zhao, Y.Q. Gao, D.P. Zhan, H. Liu, Q. Zhao, Y. Kou, Y.H. Shao, M.X. Li, Q.K. Zhuang, Z.W. Zhu, Talanta 66 (2005) 51.
[26] Q. Zhao, D.P. Zhan, H.Y. Ma, M.Q. Zhang, Y.F. Zhao, P. Jing, Z.W. Zhu, X.H. Wan, Y.H. Shao, Q.K. Zhuang, Front. Biosci. 10 (2005) 326.
[27] C.M. Li, J.F. Zang, D.P. Zhan, W. Chen, C.Q. Sun, A.L. Teo, Y.T. Chua, V.S. Lee, S.M. Moochhala, Electroanalysis 18 (2006) 713.
[28] Q.P. Yan, F.Q. Zhao, G.Z. Li, B.Z. Zeng, Electroanalysis 18 (2006) 1075.
[29] Y.J. Zhang, Y.F. Shen, J.H. Li, L. Niu, S.J. Dong, A. Ivaska, Langmuir 21 (2005) 4797.
[30] F. Zhao, X. Wu, M.K. Wang, Y. Liu, L.X. Gao, S.J. Dong, Anal. Chem. 76 (2004) 4960.
[31] Z.J. Wang, Q.X. Zhang, D. Kuehner, X.Y. Xu, A. Ivaska, L. Niu, Carbon 46 (2008) 1687.
[32] Y. Li, Y.Y. Song, C. Yang, X.H. Xia, Electrochem. Commun. 9 (2007) 981.
[33] W. Huang, Y. Wang, G.H. Luo, F. Wei, Carbon 41 (2003) 2585.
[34] Y. Wang, F. Wei, G.H. Luo, H. Yu, G.S. Gu, Chem. Phys. Lett. 364 (2002) 568.
[35] Z.Y. Du, Z.P. Li, Y.Q. Deng, Synth. Commun. 35 (2005) 1343.
[36] G. Frens, Nat.-Phys. Sci. 241 (1973) 20.
[37] X.C. Tan, M.J. Ll, P.X. Cai, L.J. Luo, X.Y. Zou, Anal. Biochem. 337 (2005) 111.
[38] A.S. Ben, Z. Dursun, T. Koga, G.S. Bang, T. Sotomura, I. Taniguchi, J. Electroanal. Chem. 567 (2004) 175.